

# Lumped Model for the Assessment of the Thermal and Mechanical Response of LNG Tanks Exposed to Fire

Giordano E. Scarponi<sup>a</sup>, Gabriele Landucci<sup>\*b</sup>, Federica Ovidi<sup>b</sup>, Valerio Cozzani<sup>a</sup>

<sup>a</sup>LISES - Dipartimento di Ingegneria Civile, Chimica, Ambientale e dei Materiali, Alma Mater Studiorum - Università di Bologna, via Terracini n.28, 40131 Bologna, Italy

<sup>b</sup>Dipartimento di Ingegneria Civile e Industriale, Università di Pisa, Largo Lucio Lazzarino 2, 56126 Pisa, Italy  
[gabriele.landucci@unipi.it](mailto:gabriele.landucci@unipi.it)

Fires may impact on liquefied natural gas (LNG) process and storage units causing severe damages and potential accident escalation. In the present work, a lumped model able to predict the thermal response of LNG tanks exposed to fire is presented. The model is based on a thermal nodes approach, solving heat and material balances on the equipment exposed to fire, contemplating boiling regime phenomena, heat-up and pressure build up. The model allowed obtaining key indications for the evaluation of the vessel resistance during fire exposure. The model was applied to reproduce the accident scenario occurred at Tivissa (Spain) in 2002 and applied to an industrial case study.

## 1. Introduction

Liquefied natural gas (LNG) was recently proposed as a low-environmental impact fuel for ships and trucks. Several projects are developed in Europe concerning the realization of LNG distribution networks in ports and in fuel stations. Past accident analysis evidences that external fires might affect LNG tanks leading to their catastrophic failure (Bonilla et al. 2012). Therefore, modelling the pressure build up and the thermal response of LNG tanks exposed to fire is of utmost importance for the prevention of major accidents and the safety of LNG distribution chains.

In the literature, several numerical (D'Aulisa et al., 2014) and experimental studies (Moodie, 1988) documented the performance of insulated (Landucci et al., 2009) and uninsulated (Birk, 1988) liquefied petroleum gas tanks. However, few studies were dedicated to LNG. Havens and Venart (2008) analysed the fire performance of moss spheres insulated with polystyrene foam using a mono-dimensional transient model. More complex dedicated approaches are still lacking. In the present work, a lumped model based on a thermal nodes approach is developed in order to support dynamic simulation of pressure build up and temperature behaviour of LNG tanks under fire attack. Specific subroutines are included in the model to account for complicating phenomena associated to the liquid boiling regime and possible discharge from emergency relief devices. In order to assess the model potentiality, simulations are carried out to reproduce the accident occurred at Tivissa (Spain) in 2002 (Planas-Cuchi et al., 2004) and to relevant industrial case studies.

## 2. Model description

The thermal model is aimed at reproducing the heat up and consequent pressurization of LNG tanks, contemplating the presence of the insulation layer, the continuous boil-off gas discharge (BOG) and the possible opening of emergency relief venting. The model is based on a thermal nodes approach, which consists of subdividing the domain into eight nodes, as shown in Figure 1. Nodes "V" and "L" represent the vapour and the liquid space, respectively. The inner shell (S), the insulant layer (I) and the external jacket (J) are subdivided in three couples of nodes,  $S_V - S_L$ ,  $I_V - I_L$  and  $J_V - J_L$  according to the liquid-vapour interface position. In particular, the subscript V indicates the nodes representing the portion of the vessel above the liquid level, whereas the subscript L identifies those below the liquid-vapour interface. This enables the model to account for the temperature difference between the wall portion in contact with the vapour space and the one wetted by the liquid. According to the previous discretization, a set of partial differential equations is defined as

reported in Table 1. The table contains the mass balances for the V and L nodes (Eq(2) and (4)) as well as the thermal balances for all the eight tank nodes (Eq(1,3,5-10)). Mechanical energy terms due to pressure in the thermal balances for liquid and vapour are neglected. In addition, two equations, one for the pressurization and the other for the liquid level, are also considered. The liquid and vapour wetted areas ( $A_L$  and  $A_V$  respectively) and the liquid-vapour interface  $A_{LV}$  are updated at each time-step as a function of the liquid level. Since the thickness of each layer is much smaller than the vessel radius, the contact surface between each of them is considered to be the same, no matter which couple of layers is considered.

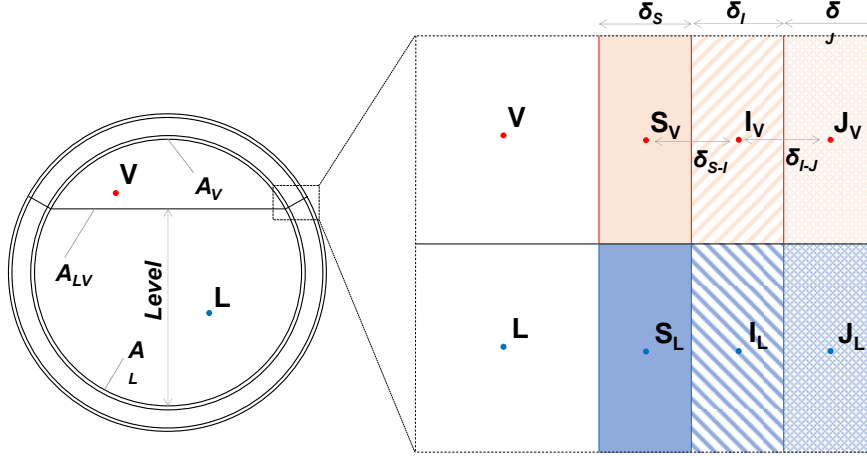


Figure 1: Schematization of thermal nodes discretization. L = liquid phase, V = vapour phase, S = shell, I = insulant, J = jacket,  $A_L$  = liquid wetted area,  $A_V$  = vapour wetted area,  $A_{LV}$  = liquid-vapour interface area.

Table 1: Thermal and mass balances for the nodes depicted in Figure 1.

Node	Variable	Equation	Eq.
L	$T_L$	$m_L cp_L \frac{dT_L}{dt} = A_L h_L (T_{SL} - T_L) + A_{LV} h_{LV} (T_V - T_L) + q_R + m_c (\hat{H}_V(T_V) - \hat{H}_L(T_L)) - m_e (\hat{H}_V(T_L) - \hat{H}_L(T_L))$	(1)
	$m_L$	$\frac{dm_L}{dt} = m_c - m_e$	(2)
V	$T_V$	$m_V cv_V \frac{dT_V}{dt} = A_V h_V (T_{SV} - T_V) - A_{LV} h_{LV} (T_V - T_L) - m_e (\hat{H}_V(T_L) - \hat{H}_V(T_V)) + \frac{RT_V}{M} \frac{dm_V}{dt}$	(3)
	$m_V$	$\frac{dm_V}{dt} = -m_c + m_e - m_{PSV}$	(4)
$S_L$	$T_{SL}$	$\delta_s \rho_{sL} cp_{sL} \frac{dT_{SL}}{dt} = -h_L (T_{SL} - T_L) + \frac{k_{S-1}}{\delta_{S-1}} (T_{IL} - T_{SL})$	(5)
$S_V$	$T_{SV}$	$\delta_s \rho_{sV} cp_{sV} \frac{dT_{SV}}{dt} = -h_V (T_{SV} - T_V) - q_R + \frac{k_{S-1}}{\delta_{S-1}} (T_{IV} - T_{SV})$	(6)
$I_L$	$T_{IL}$	$\delta_i \rho_{iL} cp_{iL} \frac{dT_{IL}}{dt} = -\frac{k_{S-1}}{\delta_{S-1}} (T_{IL} - T_{SL}) + \frac{k_{I-1}}{\delta_{I-1}} (T_{JL} - T_{IL})$	(7)
$I_V$	$T_{IV}$	$\delta_i \rho_{iV} cp_{iV} \frac{dT_{IV}}{dt} = -\frac{k_{S-1}}{\delta_{S-1}} (T_{IV} - T_{SV}) + \frac{k_{I-1}}{\delta_{I-1}} (T_{JV} - T_{IV})$	(8)
$J_L$	$T_{JL}$	$\delta_j \rho_{jL} cp_{jL} \frac{dT_{JL}}{dt} = -\frac{k_{I-1}}{\delta_{I-1}} (T_{JL} - T_{IL}) + A_L q_{FIRE}$	(9)
$J_V$	$T_{JV}$	$\delta_j \rho_{jV} cp_{jV} \frac{dT_{JV}}{dt} = -\frac{k_{I-1}}{\delta_{I-1}} (T_{JV} - T_{IV}) + A_V q_{FIRE}$	(10)
-	P	$\frac{dp}{dt} = \frac{\rho_V}{m_V} \left( \frac{P}{\rho_L} \frac{dm_L}{dt} + \frac{RT_V}{M} \frac{dm_V}{dt} + \frac{Rm_V}{M} \frac{dT_V}{dt} \right)$	(11)
-	Level	$\frac{dLevel}{dt} = \frac{1}{\rho_L} \left( \frac{dV_L}{dLevel} \right)^{-1} \frac{dm_L}{dt}$	(12)

$T$  = temperature,  $m$  = mass,  $P$  = pressure,  $V_L$  = liquid volume,  $cp$  = specific heat capacity at constant pressure,  $cv$  = specific heat capacity at constant volume,  $h$  = convective heat transfer coefficient,  $\hat{H}$  = specific enthalpy,  $R$  = gas constant,  $M$  = molecular weight,  $m_e$  = evaporation rate,  $m_c$  = condensation rate,  $m_{PSV}$  = PSV discharging rate,  $\rho$  = density,  $\delta$  = thickness,  $k$  = thermal conductivity,  $q$  = heat flux

The liquid and the vapour nodes are modelled in non-equilibrium conditions, thus considering a temperature difference between the two phases despite the pressure is uniform in the system. The evaporation and

condensation fluxes ( $m_E$  and  $m_C$  in Eq(1-4)) are defined according to the model proposed by Hertz and Knudsen equations (Knudsen, 1934):

$$m_E = A\beta_E \sqrt{\frac{M}{2\pi}} \left( \frac{p_{sat}(T_L)}{\sqrt{T_L}} \right) \quad (13)$$

$$m_C = A\beta_C \sqrt{\frac{M}{2\pi}} \left( \frac{p}{\sqrt{T_V}} \right) \quad (14)$$

In the present work, the two coefficients  $\beta_E$  and  $\beta_C$  are both assumed to be equal to  $10^{-4}$ . The other term appearing in the vapour mass balance,  $m_{PSV}$ , represents the discharging rate through the safety valve when this is open. This parameter is obtained through Eq(15,16), where  $A_{PSV}$  = discharging area,  $\gamma$  = heat capacity ratio,  $p_{out}$  = external pressure:

$$m_{PSV} = A_{PSV} p \sqrt{\frac{\gamma M}{RT_V}} \frac{Ma}{\left(1 + \frac{\gamma-1}{2} Ma^2\right)^{\frac{\gamma+1}{2(\gamma-1)}}} \quad (15)$$

$$Ma = \min \left( 1, \sqrt{\frac{\left(\frac{p}{p_{out}}\right)^{\frac{\gamma-1}{\gamma}} - 1}{\frac{\gamma-1}{2}}} \right) \quad (16)$$

Table 2: Convective heat transfer coefficients assuming natural convection before PSV opening and forced convection after PSV opening (Knudsen et al. 1999).

PSV state	Convective heat transfer coefficient	Eq.
-	$h_L = \left( 3.75 \times 10^{-5} p_c^{0.69} (T_{SL} - T_{L,sat})^{0.7} \left( 1.8 \left( \frac{p}{p_c} \right)^{0.17} + 4 \left( \frac{p}{p_c} \right)^{1.2} + 18 \left( \frac{p}{p_c} \right)^{10} \right) \right)^{3.33}$	(17)
closed	$h_V = (0.27 Ra^{0.25}) \frac{k_V}{L_V}$	(18)
open	$h_V = (0.024 Re^{0.8} Pr^{0.4}) \frac{k_V}{L_V}$	(19)
-	$h_{LV} = (0.27 Ra^{0.25}) \frac{k_V}{L_{LV}}$	(20)

$p_c$  = critical pressure,  $T_{L,sat}$  = liquid saturation temperature,  $L_V$  and  $L_{LV}$  = characteristic lengths,  $Re$  = Reynolds number,  $Ra$  = Rayleigh number,  $Pr$  = Prandtl number

The convective heat fluxes between the wall and the lading are defined by means of the heat transfer coefficients summarized in Table 2. In addition, the liquid receives heat from the shell wall in contact with the vapour in the form of radiation according to Eq (21):

$$q_R = \frac{\sigma(T_{SV} - T_L)}{\frac{1 - \epsilon_S}{\epsilon_S} A_V + \frac{1}{A_V F_{SV \rightarrow L}}} \quad (21)$$

The thermal load caused by the fire can be either assigned as a constant heat flux or defined by specifying the fire characteristics: fire temperature ( $T_f$ ) and emissivity ( $\epsilon_f$ ) and flame convective heat transfer coefficient ( $h_f$ ). In this second case, the heat flux entering the outer wall of the vessel is calculated by means of eq. 22.

$$q_{IN} = \sigma \epsilon_f (\epsilon_f T_f^4 + (1 - \epsilon_f) T_{amb}^4 - T_f^4) + h_f (T_f - T_j) \quad (22)$$

**Errore. L'origine riferimento non è stata trovata.** and Table 4 summarize the material properties adopted in the model to simulate LNG tankers. The model allows also a conservative estimation for the time to failure. This assumed to occur when the mechanical stress determined by the pressure inside the vessel equals the yield strength of the material. The Von-Mises criterion is used to evaluate mechanical stress (Landucci et al., 2009).

Table 3: Material properties considered for vapour and liquid methane (Liley et al. 1999)

Property	Symbol	Unit	Liquid methane	Vapour methane
Density	$\rho$	kg/m <sup>3</sup>	$\rho_L = \rho_L(T_L)$	Ideal gas eq.
Thermal Conductivity	$k$	W/(m·K)	$k_L = k_L(T_L)$	$k_V = k_V(T_V)$
Heat capacity	$Cp$	J/(kg·K)	$Cp_L = Cp_L(T_L)$	$Cp_V = Cp_V(T_V)$
Latent heat	$\lambda$	J/kg	$\lambda = \lambda(T)$	
Saturation temperature	$T_{sat}$	K	$T_{sat} = T_{sat}(p)$	
Viscosity	$\mu$	Pa·s	$\mu_L = \mu_L(T_L)$	$\mu_V = \mu_V(T_V)$
Surface tension	$\sigma_L$	N/m	$\sigma_L = \sigma_L(T_L)^*$	-

\* taken from <http://webbook.nist.gov/cgi/fluid.cgi?ID=C74828&Action=Page>

Table 4: Material properties considered for tank shell, insulation and jacket

Property	Symbol	Unit	AISI-304	Aluminium	Polyurethane	Perlite
Density	$\rho$	kg/m <sup>3</sup>	7800	2700	74	100
Thermal Conductivity	$k$	W/(m·K)	16	237	0.05	0.05
Heat capacity	$Cp$	J/(kg·K)	490	897	1000	838
Yield strength	$\sigma_Y$	MPa	-	220	-	-
Emissivity	$\epsilon$	-	0.9	0.9	-	-

### 3. Case studies

The first case considered is the Tivissa accident (Planas-Cuchi et al. 2004), happened in 2002, where a double-hull tanker transporting LNG lost the control and exploded due to the engulfing fire developed after the crush. The explosion occurred about 20 min after the fire started. The tank shell was made of AISI-304 stainless steel with a thickness of 4 mm. The insulation was provided by an expanded polyurethane layer (130 mm thick) with an external aluminium jacket (2 mm thick). The filling level was 85%. The tank was equipped with a total of 3 pressure safety valves (PSV). Two of them had a nominal diameter of 1" (25.4mm) and a set pressure of 7 bar. The third one, with a nominal diameter of 3/4" (19.1mm), was set at 9 bar. Planas-Cuchi et al. (2004) reported that both the crush and the subsequent fire severely damaged the insulation layer. However, no information is provided about the extent of the insulation damaging. This introduces a high degree of uncertainty in the modelling. Furthermore, the actual fire load can only be estimated from the pictures taken during the accident. For this reasons, a series of simulations was performed considering different fire loads. Moreover, in order to reproduce the deterioration in the protection performance due the damaging of the insulation, the thickness of the polyurethane layer was reduced and a higher value for the thermal conductivity was adopted. In absence of specific data for the degraded polyurethane, an indicative value of 0.3 W/(m·K) was assumed for the thermal conductivity in analogy with measurements performed by Gomez-Mares et al. (2012a) on degraded intumescent epoxy resins.

Table 5: List of case studies considered for model validation and large scale simulations.

Case study	Description	Fire load
CASE A1	Tivissa accident, intact insulation ( $k_i = 0.05$ w/(mK), $\delta_i = 0.13$ m)	100 kW/m <sup>2</sup>
CASE A2	Tivissa accident, intact insulation ( $k_i = 0.05$ w/(mK), $\delta_i = 0.13$ m)	150 kW/m <sup>2</sup>
CASE A3	Tivissa accident, intact insulation ( $k_i = 0.05$ w/(mK), $\delta_i = 0.13$ m)	200 kW/m <sup>2</sup>
CASE A4	Tivissa accident, $k_i = 0.3$ w/(mK), $\delta_i = 0.13$ m	100 kW/m <sup>2</sup>
CASE A5	Tivissa accident, $k_i = 0.3$ w/(mK), $\delta_i = 0.13$ m	150 kW/m <sup>2</sup>
CASE A6	Tivissa accident, $k_i = 0.3$ w/(mK), $\delta_i = 0.13$ m	200 kW/m <sup>2</sup>
CASE A7	Tivissa accident, $k_i = 0.05$ , $\delta_i = 0.04$ m	100 kW/m <sup>2</sup>
CASE A8	Tivissa accident, $k_i = 0.3$ w/(mK), $\delta_i = 0.04$ m	100 kW/m <sup>2</sup>
CASE B1	Cylindrical storage vessel, filling degree = 85 %	$T_f = 1000$ K, $\epsilon_f = 1$ , $h_f = 25$ W/(m <sup>2</sup> K)
CASE B2	Cylindrical storage vessel, filling degree = 50 %	$T_f = 1000$ K, $\epsilon_f = 1$ , $h_f = 25$ W/(m <sup>2</sup> K)

In addition to the Tivissa accident, the case of a cylindrical storage vessel is taken into consideration as an example of industrial storage units. Even in this case a double containment tank is considered. However, the dimension are considerably different. The internal and external shells are both made of AISI-304 stainless steel with a thickness of 26 and 30 mm respectively, the inner diameter is 6.5 m. The gap between the shells is filled by granular perlite kept in vacuum conditions, which provides thermal insulation. Unlike road tankers,

storage vessels are generally equipped with a collector for the boil-off gas in order to avoid self-pressurization due to methane evaporation. This is taken into account by considering an additional term in the mass balance for the vapour space. Table 5 summarizes the simulations performed. In the case of the storage tank, two different filling levels are considered, in order to test the influence of this operating variable on the vessel response.

#### 4. Results and discussion

Figure 2a shows the pressurization rate obtained for the case study CASE A1 to CASE A8. The yellow curves (CASE A1 to A3) clearly shows that if the thermal protection is not damaged, the pressurization is very slow and, even for the worse fire scenario (CASE A3,  $200 \text{ kW/m}^2$  heat load), the pressure inside the vessel after 1h of fire engulfment is still far from causing the PSV opening. The pressure behaviour substantially changes when polyurethane degradation is taken into account. The blue lines show the results obtained keeping the design thickness, but assuming a thermal conductivity equal to  $0.3 \text{ W/(mK)}$  for the degraded insulation layer (CASE A4 TO A6). The pressurization is much faster, causing the vessel failure in around 42 min for the less severe fire scenario (CASE A4) and about 10 min earlier for the most severe one (CASE A6). Similar results are obtained when a 70 % reduction of the insulation layer thickness is assumed, keeping a thermal conductivity of  $0.05 \text{ W/(mK)}$  (CASE A7). However, failure time as short as the one observed in the Tivissa accident can only be observed by simulating the insulant degradation both reducing the thickness reduction increasing the thermal conductivity (CASE A8). The red line in Figure 2a shows that, in this last case, the model predicts the vessel failure within about 20min. Considering the behaviour of the PSVs, it appears that they are undersized, at least for the fire scenario assumed. In fact, they do not ensure the appropriate discharging rate to stop or significantly delay pressurization.

Figure 2b reports the temperature behaviour of the liquid (blue dashed line) and vapour (red continuous line) nodes for CASE A4. The chart highlights the temperature difference between the two phases due to the non-equilibrium conditions. It is also worth noticing that the model is able to reproduce the cooling effect produced by the vapour expansion determined by PSV opening. This is evident in the behavior of the red continuous line in Figure 2b between 20 and 30 min after the fire ignition.

For what concerns the case of the cylindrical storage vessel with intact insulation, the model indicates that 1h of exposure to the fire load indicated in Table 5 is not enough to cause vessel pressurization, e.g. for both CASE B1 and B2. This is due to the high degree of protection offered by the cryogenic thermal insulation thickness. As shown in Figure 3 (obtained for CASE B1), despite the external shell reaches the fire temperature after about 30 min, the inner wall remains at extremely low temperatures. The change in the filling degree does not provide any appreciable difference in the results obtained for the two cases under consideration. It is worth noticing that the boil-off gas collector itself behaves as depressurization device, slowing down the pressure build up. However, as evidenced by the analysis of the Tivissa accident, the damage and deterioration of the heat insulation layer may have a relevant impact on the thermal protection, as documented by several experimental studies carried out on organic (Gomez-Mares et al., 2012b) and inorganic (Moricone and Tugnoli, 2015) passive fire protection materials

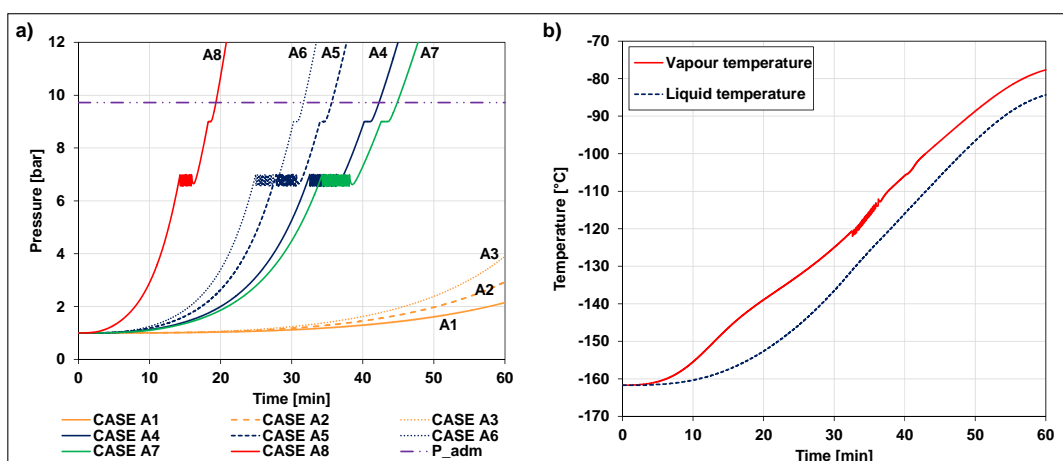


Figure 2: Pressurization curves for CASE A1 to A8 (a) and temperature behaviour for the vapour and liquid node for CASE A4 (b). For cases definition, see Table 5.

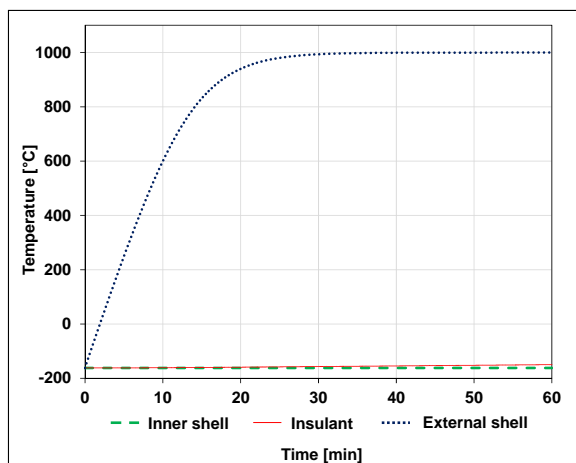


Figure 3: Inner shell, insulant and external shell temperatures as function of time for CASE B1 (see Table 5).

## 5. Conclusions

The problem of predicting the thermal response of LNG tanks exposed to fires was addressed by developing a lumped model based on thermal nodes discretization. The model application to a real accident scenario showed that such approach provides a conservative but realistic prediction of the pressure build up, as well as the transient heating of the vessel wall and its lading. Slow pressurization rates were registered simulating the case of road tankers and storage tanks with undamaged insulation. Hence, the insulation system designed with the aim of minimizing the evaporation rate of the LNG in cryogenic conditions represents also an effective protection against fire attack. However, when the insulation layer is damaged, this protection drastically depletes, jeopardizing the vessel integrity in case of fire. The lumped modelling approach may constitute a starting point for more advanced simulation studies based on distributed parameters codes (D'Aulisa et al., 2014).

## Reference

- Birk A.M., 1988, Modelling the response of tankers exposed to external fire impingement, *J. Hazard. Mater.*, 20, 197-225.
- Bonilla J.M., Belmonte, J., Marín, J.A., 2012, Analysis of the explosion of a liquefied-natural-gas road tanker, *Seguridad Y Medio Ambiente. Fundacion Mapfre*, 1-20.
- D'Aulisa A., Tugnoli A., Cozzani, V., Landucci, G., Birk, A.M., 2014. CFD modeling of LPG vessels under fire exposure conditions. *AIChE Journal*, 60(12), 4292–4305.
- Gomez-Mares M., Tugnoli A., Landucci G., Barontini F., Cozzani V., 2012a, Behavior of Intumescent Epoxy Resins in Fireproofing Applications, *J. Analyt. App. Pyrolysis*, 97, 99–108.
- Gomez-Mares M., Tugnoli A., Landucci G., Cozzani V., 2012b, Performance assessment of passive fire protection materials, *Ind. Eng. Chem. Res.*, 51, 7679–7689
- Havens J., Venart, J., 2008, Fire performance of LNG carriers insulated with polystyrene foam, *J. Hazard. Mater.*, 158 (2-3), 237-279.
- Knudsen, 1934, *The kinetic theory of gases. Some modern aspects*, Methuen and Co., Ltd., London, UK.
- Knudsen J.G., Hottel H.C., Sarofim A.S., Wankat P.C., Knaebel K.S., 1999, Heat and Mass Transfer, in: Perry RH, Green DW, editors. *Perry's Chemical Engineers' Handbook*, 7th ed., McGraw-Hill, New York, NY.
- Landucci G., Molag M., Reinders J., Cozzani V., 2009, Experimental and analytical investigation of thermal coating effectiveness for 3m<sup>3</sup> LPG tanks engulfed by fire, *J Hazard. Mater.* 161(2–3), 1182–1192.
- Liley P.E., Thomson G.H., Friend D.G., Daubert T.E., Buck E., 1999, Physical and Chemical Data, in: Perry RH, Green DW, editors. *Perry's Chemical Engineers' Handbook*, 7th ed., McGraw-Hill, New York, NY.
- Moodie K., 1988, Experiments and modelling: an overview with particular reference to fire engulfment, *J. Hazard. Mater.*, 20, 149–175.
- Moricone R., Tugnoli A., 2015, Investigating the properties of fireproofing materials for an advanced design of equipment protection, *Chemical Engineering Transactions*, 43, 2389-2394 DOI: 10.3303/CET1543399
- Planas E., Nùria G., Ventosa A., Casal J., 2004, Explosion of a road tanker containing liquified natural gas, *Journal Loss Prev. Proc. Ind.*, 17, 315–321.